Call for GSA Connects 2023 Proposals

GSA TODAY

THE GEOLOGICAL SOCIETY OF AMERICA®

VOL. 32, NO. 12 | DECEMBER 2022

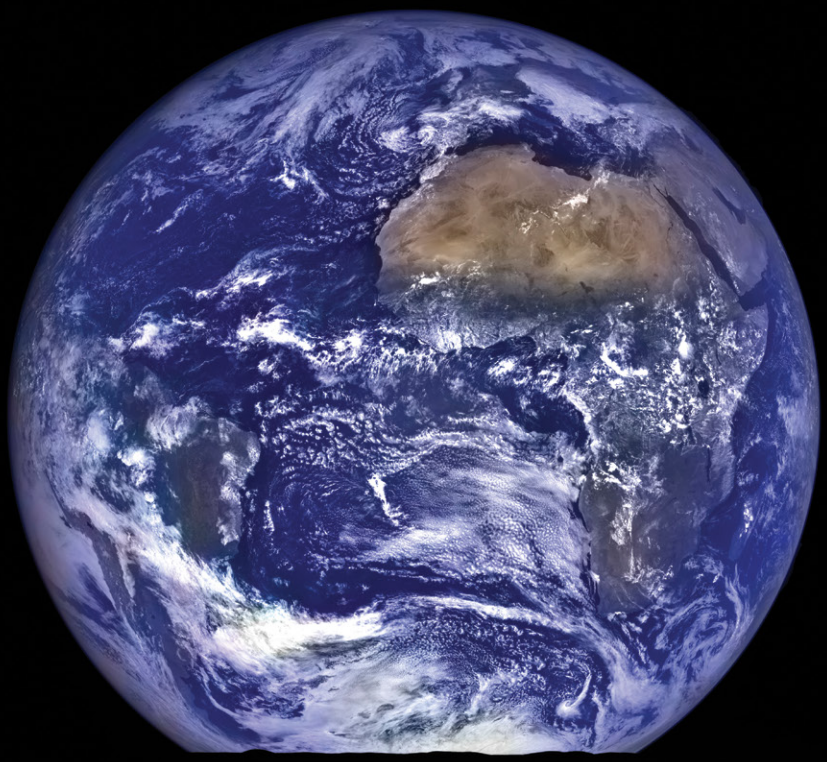

Biotic Enhancement of Weathering over the Past 3.7 Billion Years

THE GEOLOGICAL SOCIETY OF AMERICA®

Biotic Enhancement of Weathering over the Past 3.7 Billion Years

Gregory J. Retallack, *Dept. of Earth Sciences, University of Oregon, Eugene, Oregon 97403-1272, USA, gregr@uoregon.edu*

ABSTRACT

Over the past four billion years, our sun became 30% brighter, yet Earth's water has neither completely frozen nor boiled off during that time. A theoretical solution to this paradox is a carbon dioxide greenhouse planetary thermostat regulated by evolutionary advances in biologically mediated silicate and apatite weathering. This carbon sequestration history can now be quantified using paleosols. Calculations of precipitation-normalized nutrient depletion rates (μmol mm^{-1} a^{-1}) in paleosols ranging in age back to 3.7 Ga show discrete order of magnitude increases in carbon consumption by silicate and apatite weathering due to evolutionary advances in life on land at around the Great Oxidation Event (2.45 Ga) and Neoproterozoic Oxidation Event (0.8 Ga). This biological weathering countered increased solar luminosity and continued emission of volcanic greenhouse gases.

INTRODUCTION

The faint young sun paradox arises from stellar evolution of increased solar luminosity through time (Ribas, 2009), which predicts frigid temperatures on early Earth, with or without present atmosphere (Fig. 1). However, moderate Archean temperatures are inferred from salt stability, water-lain sedimentary structures, and glacial episodes (Walker, 1982). Paleotemperatures from paleosols (Fig. 1) are evidence of long-term stability (Retallack, 2013, 2018; Retallack et al., 2016), averting terminal freezing, apparent from Mars, as well as the other extreme of an uninhabitable inferno, apparent from Venus (Lovelock and Margulis, 1974). Both freezing and steaming may have been prevented by greenhouse gases such as CH_4 and CO_2 regulated by the biological carbon cycle (Schwartzmann, 2017). Continued volcanic degassing of CO_2 prevented a terminal icehouse, whereas building of biomass and consumption of carbonic acid by biotically enhanced silicate and apatite weathering prevented a terminal greenhouse (Retallack, 2022a). Consumption of CO_2 by abiotic silicate weathering in lifeless Precambrian landscapes was modeled by Rye and Holland (1998), but a role for life on land enhancing weathering is indicated as far back as 3.7 Ga by paleosol salts, stable isotopic compositions, and phosphorus depletion (Retallack, 2022b). Thus, theoretical concepts of biotic planetary temperature regulation can now be assessed from the record of fossil soils back to 3.7 Ga. Generally declining atmospheric CO_2 over time (Kasting, 2010) is not the only issue involved, because soil CO_2 increased with increased productivity of terrestrial vegetation (Retallack, 2022b). Paleosols are not only evidence of carbon sequestration by silicate and apatite weathering, but also include fossils as evidence of the evolution of life on land.

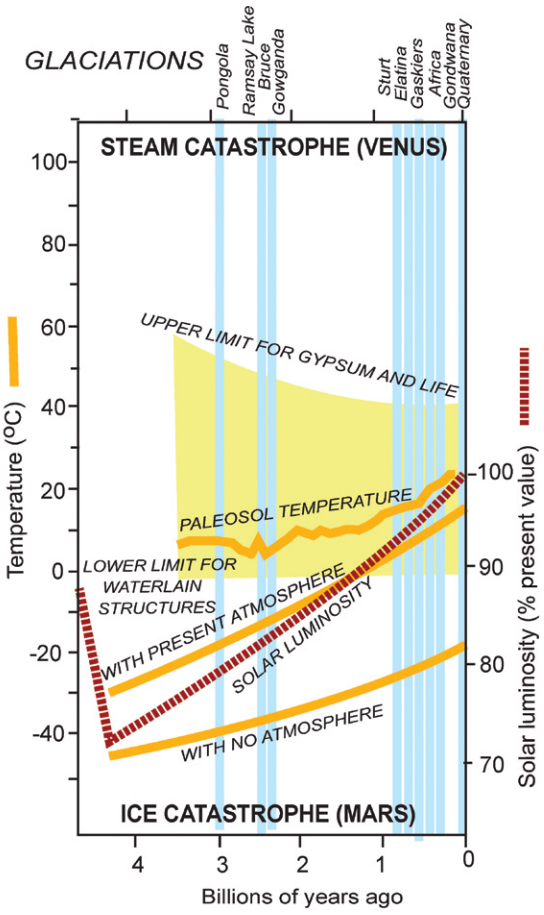

Figure 1. Stellar evolution and planetary temperature and atmospheric composition over the past 4.6 Ga, showing solar luminosity increase and predicted temperature of Earth with current atmosphere or no atmosphere (Ribas, 2009), envelope of permitted temperatures from gypsum and life (Walker, 1982), temperatures inferred from selected paleosols (Retallack, 2013, 2018; Retallack et al., 2016), and ice ages (Walker, 1982).

PALEOSOLS AS PROXIES FOR CARBON SEQUESTRATION

Paleosols are soils of the past, buried in sedimentary or volcanic sequences, and interpretable by comparison with modern soils. Release of soluble alkali and alkaline earth cations and bicarbonate into soil solution by carbonic acid from CO_2 in solution

GSA Today, v. 32, https://doi.org/10.1130/GSATG543A.1. CC-BY-NC.

can be simplified to Equations 1–4, showing that each mole of oxide consumed 2 moles of CO_2:

$$MgO + 2CO_2 + H_2O \rightarrow Mg^{2+} + 2HCO_3^-, \quad (1)$$

$$CaO + 2CO_2 + H_2O \rightarrow Ca^{2+} + 2HCO_3^-, \quad (2)$$

$$Na_2O + 2CO_2 + H_2O \rightarrow 2Na^{+} + 2HCO_3^-, \quad (3)$$

$$K_2O + 2CO_2 + H_2O \rightarrow 2K^{+} + 2HCO_3^-. \quad (4)$$

Losses of these elements from soils on a molar basis is a proxy for moles of CO_2 consumed by soil over its time of formation (Sheldon, 2006). Whole profile loss can be envisaged as the area under the curves in mole fraction alkali and alkaline earth depletion for decompacted paleosols (Fig. 2).

Dissolution of apatite as a source of P can be reduced to Equation 5, in which 1 mol of CO_2 in aqueous solution liberates 3 moles of soluble phosphate from apatite:

$$Ca_5(PO_4)_3(OH) + CO_2 \rightarrow 5Ca^{2+} + 3PO_4^{3-} + HCO_3^- \quad . \quad (5)$$

This is a simplification of four intermediate apatite dissolution reactions and other intermediate reactions producing carbonic acid from CO_2 in solution (Dorozhkin, 2012). Actual phosphate procurement in soils from relatively insoluble apatite is catalyzed by a variety of carbon-based acid moieties, such as acetic and oxalic acid with higher mole fractions of carbon (Neaman et al., 2005). Another complication is that Archean apatite dissolution also may have been partly achieved by strong sulfuric acid, rather than weak carbonic acid (Retallack, 2022c). Again, this is based on mass transfer, including volume loss during soil formation with depth in reconstructed soils as they would have been before burial compaction and metamorphism (Sheldon, 2006).

Original soils can be reconstructed from paleosols by estimating compaction due to burial by overburden (C as %) from total depth of burial (B in km) and suitable physical constants, in this case taken from Aridisols (Sheldon and Retallack, 2001):

$$C = \frac{-0.51 \times 100}{\left\{ \left(\frac{0.49}{\frac{B}{e^{0.27}}} \right) - 1 \right\}} \quad . \quad (6)$$

Tau analysis of paleosols (Brimhall et al., 1992) calculates mole fraction mass transport ($\tau_{j,w}$) of a mobile element and mole fraction strain ($\varepsilon_{i,w}$) of the profile during soil formation using an immobile element from the parent material (Ti used here). Equations 7–8 for mass transport and strain include bulk density (ρ in g.cm^{-3}) and oxide assay (C in wt%) for successive samples (subscripts i, j) of weathered material (subscript w) and parent material (subscript p) of a single paleosol profile:

$$\varepsilon_{i,w} = \left[\frac{\rho_p C_{j,p}}{\rho_w C_{j,w}} \right] - 1, \quad (7)$$

$$\tau_{j,w} = \left[\frac{\rho_w C_{j,w}}{\rho_p C_{j,p}} \right] \left[\varepsilon_{i,w} + 1 \right] - 1. \quad (8)$$

Soils and paleosols lose mass with weathering and so have negative strain ($\varepsilon_{i,w} < 0$), and also lose nutrient cations and silica, so have negative mass transfer ($\tau_{j,w} < 0$). In contrast, sediment accumulation and diagenetic alteration add elements and mass, so have positive strain and mass transfer. Moles of CO_2 used to displace alkali and alkaline earths during weathering assessed by tau analysis (Equations 7–8) can be used to calculate soil CO_2 (ppm) consumed by the whole profile during its formation using Equations 9–11 (modified from Sheldon, 2006). Components of these calculations are areas under the curves of depletion of bases or phosphorus in reconstructed paleosol profiles, calculated for the whole profile for a square centimeter of surface area of the profile (Fig. 2):

$$pCO_2 = \frac{F}{A\left[\frac{K_{CO_2} P}{1000} + \kappa \frac{D_{CO_2} \alpha}{L} \right]}, \quad (9)$$

$$F = 2\sum \rho_p \frac{C_{j,p}}{100} \int_{Z=0}^{Z=D_{j,w}} \tau_{j,w(z)} \delta Z \quad , \quad (10)$$

$$G = 5\sum \rho_p \frac{C_{j,p}}{100} \int_{Z=0}^{Z=D_{j,w}} \tau_{j,w(z)} \delta Z \quad . \quad (11)$$

Variables and constants for these calculations besides those needed for Equations 6–8 are F (mol CO_2.cm^{-2}) = summed molar mass transfer loss of CaO, MgO, Na_2O, and K_2O using Equation 9; G (mol CO_2.cm^{-2}) = summed molar mass transfer loss of P using Equation 10; Z (cm) = depth in soil represented by analysis corrected for compaction using Equation 10; A (years) = duration of soil formation using Equations 12 and 13; K_{CO_2} (mol./kg.bar) = Henry's Law constant for CO_2 (=0.034, range 0.031–0.0045); P (cm) = mean annual precipitation using Equation 13; κ (s.cm^3.[mol.year]$^{-1}$) = seconds per year divided by volume per mole of gas at standard temperature and pressure (=1430);

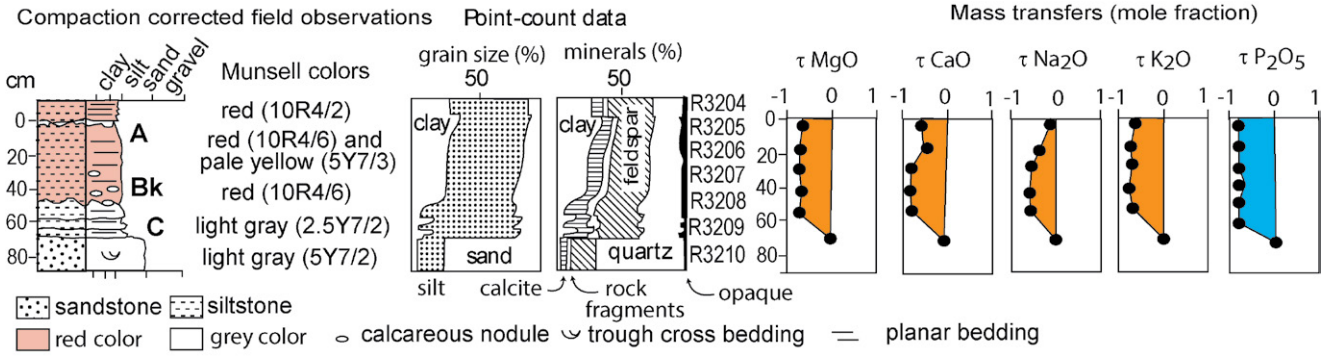

Figure 2. Base and phosphorus depletion in a 550 Ma paleosol from South Australia as an example of output data for each reconstructed paleosol. Parent material was chosen on the basis of petrographic, titania, and sesquioxide similarity detailed elsewhere (Retallack, 2013).

D_{CO_2} ($cm^2.s^{-1}$) = diffusion constant for CO_2 in air (=0.162); α (fraction) = ratio of diffusion constant for CO_2 in soil divided by diffusion constant for CO_2 in air (=0.1, range 0.08–0.12); *L* (cm) = original depth to water table (after decompacted using Equation 6).

The duration of soil formation in years (*A* in k.y.) can be calculated from carbonate nodule diameter (*D* in cm: $r^2 = 0.57$, s.e. = 1.8, p = <0.001) for calcareous soils (Retallack, 2005), or thickness of profile (*T* in cm: $r^2 = 0.79$, s.e. = 140, p = 0.01) for non-calcareous unconformity paleosols (Markewich et al., 1990):

$$A = 3.92D^{0.34}, \quad (12)$$

$$A = 4.915T - 343.4. \quad (13)$$

Mean annual precipitation (*P* in mm) can be obtained by the CIA-K proxy, effectively a chemical index of alteration without diagenetically problematic K (*I* as mole fraction: $r^2 = 0.72$, s.e. = 182, p = <0.0001; Sheldon et al., 2002), or compaction-corrected depth to calcic horizon (*D* in cm: $r^2 = 0.52$, s.e. = 147, p = <0.0001; Retallack, 2005):

$$P = 221.1e^{0.0197I}, \quad (14)$$

$$P = 137.24 + 6.45D - 0.0132^2. \quad (15)$$

The normalized value of μmol *F*.cm^2.mm^{-1}.a^{-1}, where *F* is the sum of the four alkaline and alkaline earth bases, or μmol *G*.cm^2.mm^{-1}.a^{-1}, where *G* is the sum of phosphorus depletions, become proxies for global CO_2 consumption if multiplied by modal mean annual precipitation, which is 764 mm in the modern world, with a standard error of 704 mm (Beck et al., 2005). This modal mean annual precipitation may have changed in deep time, but the current understanding of paleoprecipitation from paleosols shows mainly arid to subhumid estimates (Retallack, 2013, 2018; Retallack et al., 2016), comparable with today (Beck et al., 2005). Estimates of exposed land area in deep time are from published areas of continental crust and hypsometric curves (Cawood and Hawkesworth, 2019). These changing land areas were proportionally scaled to a modern land area of 148,429,000 km^2, and carbon consumption to modern global silicate weathering (Ciais et al., 2013) of 0.3 PgC.a^{-1} (Pg = 10^{15}g). Carbon consumption by silicate weathering can be calculated from stoichiometry of Equations 1–4 and carbon consumption by apatite weathering from stoichiometry of Equation 5.

DATABASE, ERROR CALCULATIONS, AND ALTERNATIVES

Detailed accounts of each of the paleosols used in the compilation for these calculations have all been published elsewhere: citations and component data, including error estimates for individual profiles, are listed in the supplemental material[1]. Criteria for quality of data outlined by Rye and Holland (1998) were used to select paleosols for the compilation. Full petrographic and geochemical data, as well as bulk density determinations, were essential for all horizons (Equations 7 and 8). Also needed was evidence of at least moderate development, such as argillic, calcic, or gypsic horizons (Retallack, 2013, 2018, 2022b). To be included, paleosols had to have chemical weathering demonstrated by tau analysis (Brimhall et al., 1992). Weakly developed, gleyed, and inadequately documented paleosols were not included. The paleosol database includes profiles on bedrock unconformities (Rye and Holland, 1998), as well as within sedimentary sequences (Retallack, 2013, 2018, 2022b). Virtually all suitable Precambrian paleosols are included in the database, along with most suitable Phanerozoic paleosols for which data was available. Errors for the calculations were based on standard errors of transfer functions (Equations 12–15) and Gaussian error propagation from partial derivatives of transfer equations summed in quadrature as outlined by Retallack et al. (2021).

Some of the transfer functions used are compromised by other variables: Equations 14 and 15 for paleoprecipitation include components of temperature (Sheldon et al., 2002) and paleoproductivity, respectively (Breecker and Retallack, 2014), which contribute to cited standard errors. Warmth and high precipitation can also compromise age estimates of paleosols using nodule size (Retallack, 2005) and depth of weathering (Markewich et al., 1990), again within standard error of the data used for the transfer function. Although individual paleosol depletion rate standard deviations were small, the variance of estimated depletion rates is large, so rates were pooled by 500-m.y. increments to calculate standard deviations as the height of the open box (Fig. 3).

STEPWISE BIOTIC ENHANCEMENT OF WEATHERING

The results of mass transfer calculations of paleosols ranging back in age to 3700 Ma show three orders of magnitude increases in nutrient depletion of both phosphorus and alkali and alkaline earths, but on different time schedules (Figs. 3A–3B). Most of the range of alkali and alkaline earth depletion was achieved by the Great Oxidation Event (GOE) of 2.45 Ga, but phosphorus depletion rose markedly at both the GOE and the Neoproterozoic Oxidation Event (NOE) of 0.8 Ga. These changes may reflect increased rates of nutrient procurement due to increased biological productivity at those times.

Alkali and alkaline earth depletion rose steadily from 3.5 to 2.4 Ga under acid-sulfate weathering by anaerobic bacterial soil microbiomes (Retallack, 2018; Retallack et al., 2016), now restricted to waterlogged soils and playa lakes (Benison and Bowen, 2015). Alluvial paleosols from 3.5 to 3.0 Ga contain desert roses of sulfate minerals, such as barite and gypsum, as evidence for weathering by strong sulfuric acid rather than weak carbonic acid (Retallack, 2018; Retallack et al., 2016). The microbiome of desert rose paleosols dated to 3.0 Ga is permineralized with silica, and its microfossils, analyzed for cell-specific carbon-isotopic-composition, reveal an anaerobic community of purple sulfur bacteria, actinobacteria, and methanogens (Retallack et al., 2016).

Other paleosols in the data set formed in humid climates on bedrock (supplemental material [see footnote 1]) and were thick, clayey profiles, with little evidence of soluble salts (Rye and Holland, 1998). These do not stand out as anomalies in Figure 3 compared with paleosols with soluble salts (Retallack, 2022c) because they were normalized for mean annual precipitation (Equations 12–13) and duration of formation (Equations 14–15). CO_2 consumption rates of Paleoproterozoic and Archean paleosols are too low (Fig. 4) to explain paleotemperatures under a faint young sun (Kasting, 2010). Likely sulfur bacteria and methanogens in paleosols support the idea that other greenhouses gases, such as methane, ethane, and SO_2, formed a greenhouse

[1]Supplemental Material. Table S1. Base and phosphorus depletion and paleoenvironments of 97 well-studied paleosols. Go to https://doi.org/10.1130/GSAT.S.20126417 to access the supplemental material; contact editing@geosociety.org with any questions.

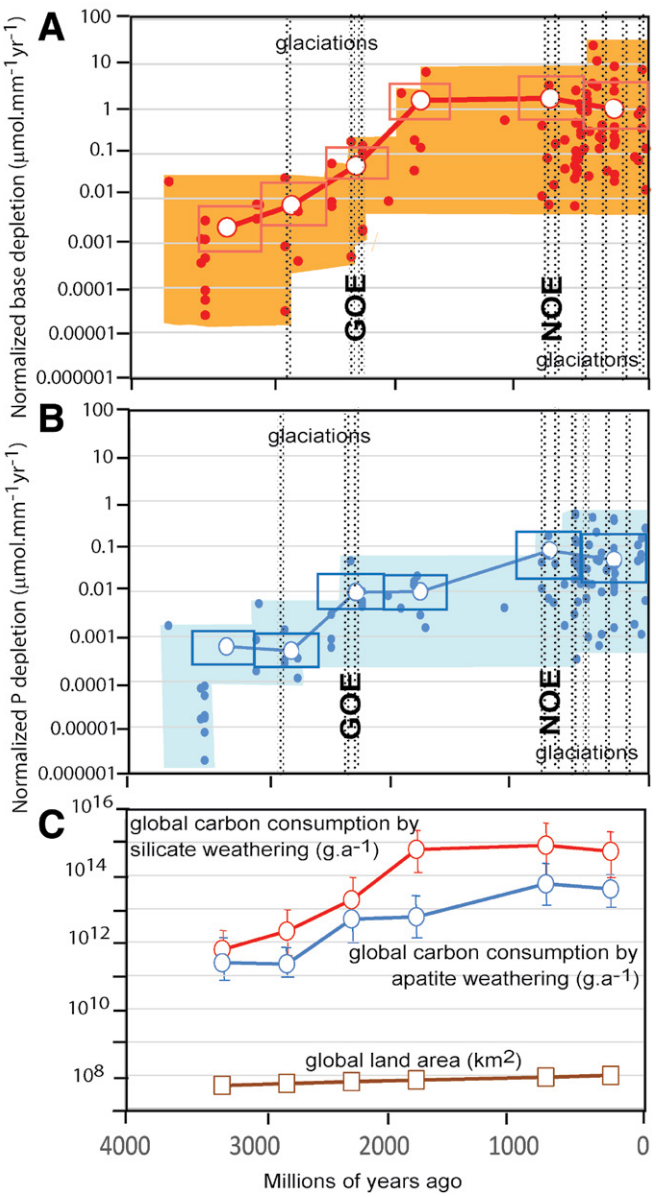

Figure 3. Base (A) and phosphorus depletion (B) and carbon consumption (C) inferred from tau analysis of paleosols over the past 3.7 Ga. (A–B) Closed symbols are individual paleosols, and large open symbols are mean for 500 Ma intervals. Only a single paleosol is known for 1000–500 Ma. (C) Annual rates of C consumption from base depletion and apatite weathering (see supplemental material [see text footnote 1]) and global land area increase calculated from continental area and freeboard estimates (Cawood and Hawkesworth, 2019). Upper and lower box bounds and error bars are two standard deviations. GOE—Great Oxidation Event; NOE—Neoproterozoic Oxidation Event.

haze (Haqq-Misra et al., 2008). Modeling of methane production rates from a P-limited and SO_4-poor Archean ocean would not have produced enough methane for a significant CH_4-greenhouse (Laakso and Schrag, 2019), but anaerobic methanogenesis would have been more widespread in well-drained Archean soils than its current geographic limitation to waterlogged wetlands (Benison and Bowen, 2015). Another Archean warming possibility is three times the current mass of atmospheric N_2 and a H_2 0.1 mixing ratio (Wordsworth and Pierrehumbert, 2013). This seems unlikely because N_2 in the atmosphere was limited to 1.1–0.5 bars judging from nitrogen and argon isotopic ratios in fluid inclusions dated to 3500 Ma (Marty et al., 2013), and total atmospheric pressure at 2700 Ma may have been only half modern judging from the size of lava vesicles and raindrop impressions (Som et al., 2016).

The Archean acid-sulfate weathering style was geographically limited by late Archean spread of carbonic acid weathering, which dominated after the 2.45 Ga GOE (Rye and Holland, 1998). The rise of cyanobacteria as part of a largely freshwater and terrestrial clade of "Terrabacteria" (Battistuzzi and Hedges, 2009) maintained soil productivity, promoting perineutral carbonic acid hydrolysis and free oxygen in both soil and air (Fig. 4). Perineutral pH in soils by 2.4 Ga is indicated by pedogenic carbonate in paleosols of that age and in aridland soils ever since (Pekkarinen, 1979). Thus, hydrolytic weathering systems geographically displaced archaic acid-sulfate weathering, now limited to areas of sulfide ore weathering and anaerobic parts of waterlogged soils and lakes (Benison and Bowen, 2015).

Phosphorus depletion of paleosols rose during the GOE, and again during the NOE (Fig. 3B). The Neoproterozoic does not signify a fundamental change in style of weathering, but rather the evolution of more effective biologically produced ligands, which were mainly bacterial during the GOE, but supplemented by more effective ligands of fungi and lichens during the Neoproterozoic (Neaman et al., 2005; Retallack, 2013; Kump 2014). Both increases in terrestrial productivity coincide in time with Snowball Earth cooling events (Walker, 1982; Kasting, 2010).

IMPLICATIONS FOR SOIL GASES IN DEEP TIME

Some of these same paleosols also have been used to calculate CO_2 consumption as a guide to atmospheric evolution (Sheldon, 2006; Retallack et al., 2021), but they are imperfect guides to the atmosphere. Today, soils may have up to three orders of magnitude more CO_2 than the atmosphere because of soil respiration, and three orders of magnitude less O_2 due to waterlogging (Elberling et al., 2011). The differences in CO_2 and O_2 from the atmosphere are less marked in well-drained soils with open-soil structure (Kyaw Tha Paw et al., 2006). Calculations of gas consumption from paleosols (Sheldon, 2006; Retallack et al., 2021), combined with modern soil gas measurements (Elberling et al., 2011; Kyaw Tha Paw et al., 2006), allow idealized hypotheses for gas concentrations within well-drained alluvial soils over the past 3.7 billion years (Fig. 4). Both O_2 and CO_2 are higher in modern than in Precambrian soils, and geologically younger

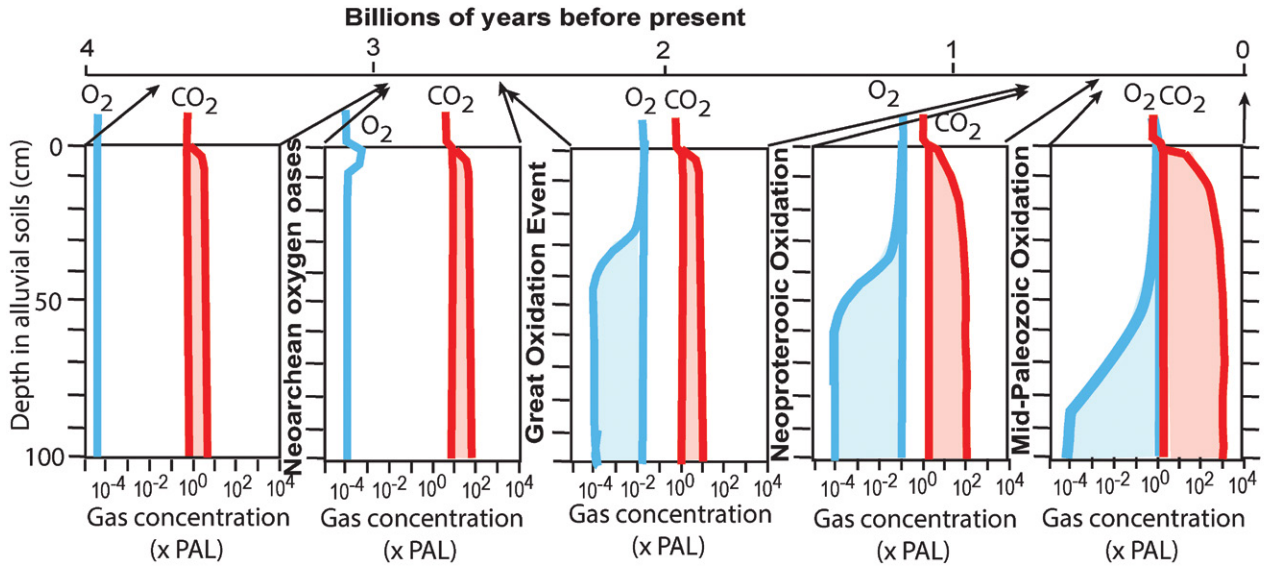

Figure 4. Idealized range of soil gas distributions on Earth over the past 4 billion years. Gas concentrations varied within the envelope shown depending on seasonal productivity and waterlogging, and atmospheric levels of gases inferred from paleosol consumption are shown at the surface. PAL—preindustrial atmospheric level (280 ppm).

soils show more variable concentrations with seasons, within profiles, and geographically (Breecker and Retallack, 2014). Thus, biotic enhancement of weathering was not just a matter of changing the atmosphere (Kasting, 2010), because soil gases at the site of silicate and apatite weathering were critical (Kump, 2014). Neoproterozoic consumption of CO_2 was less by increased silicate weathering than by increased apatite weathering (Fig. 3), suggesting a role for ligands from life on land (Neaman et al., 2005). With later evolution of land plants, soil CO_2 rose orders of magnitude higher than in the atmosphere, supplying carbonic acid for both silicate and apatite weathering (Berner, 1997; Retallack, 2022a, 2022b).

Estimates of CO_2 consumption by Paleoproterozoic and Archean soils do not show expected (Kasting, 2010) high amounts of soil or atmospheric CO_2 (Sheldon, 2006; Retallack, 2018; Retallack et al., 2016, 2021). Common sulfates formed in Archean paleosols despite low atmospheric O_2 suggest that strong sulfuric acid produced by anaerobic sulfur oxidizing bacteria, creating more amorphous colloids such as imogolite than clay, may have been more important than weak carbonic acid in Archean silicate weathering (Retallack, 2018; Retallack et al., 2016). Paleoproterozoic atmospheric oxidation raised rates of atmospheric CO_2 consumption by both oxidative silicate and apatite weathering from aerobic cyanobacteria and actinobacteria, but increases in apatite, not silicate, weathering rates are seen in the Neoproterozoic (Fig. 3), perhaps from newly evolved fungal-lichen microbial earths (Retallack, 2013; Kump, 2014). The advent of land plants did draw down atmospheric CO_2 (Berner, 1997) but did not appreciably alter rates of CO_2 consumption by either silicate or apatite weathering at the coarse 500-m.y. scale of this investigation (Fig. 3). During the past 16 million years, range expansion and contraction of carbon-hungry soils such as Mollisols and Oxisols, with reciprocal adjustment of carbon-lean soils such as Gelisols and Aridisols have acted as a planetary thermostat. Mollisol-Oxisol expansion curbs greenhouse CO_2 spikes, but Gelisol-Aridisol expansion cannot override continued volcanic degassing of CO_2 (Retallack, 2022a). Too few Archean paleosols are now known to demonstrate such counterbalancing carbon sequestration, but biotic enhancement of weathering is suspected then as well. The record of paleosols reveals that atmospheric and soil CO_2 show considerable temporal and presumably also geographic variation (Fig. 3) but not a monotonic increase (Fig. 4). Nevertheless, carbon sequestration by silicate weathering and phosphorus depletion did rise (Fig. 4), as predicted in theory (Schwartzmann, 2017).

COMPARISON WITH EXPERIMENTS

Increases of three orders of magnitude in nutrient depletion of individual paleosols (Fig. 3A) and global carbon sequestration (Fig. 3C) is greater than an estimate of two orders of magnitude of biotic enhancement of weathering derived from compilation of experimental studies (Schwartzmann, 2017) for three reasons. First, experimental studies reveal enhancement factors of major steps in terrestrial productivity, such as the evolution of trees (Retallack, 2022b), and does not consider the origin of microbial life in soils and prokaryotic evolutionary advances in microbiome weathering. Second, global carbon sequestration has been aided by the growth of land area through time. The estimates of land-area increase used here are based on estimates of continental area and paleohypsometry (Cawood and Hawkesworth, 2019), which are relatively conservative, but show a factor of three, rather than a factor of 100 increase through time (Fig. 3C). Third, nutrient depletion fuels biomass carbon sequestration increases of about the same magnitude (Retallack, 2022a). Geographic spread and temporal fluctuation in areas of various kinds of paleosols will be needed for a full accounting of planetary temperature regulation by soils, as has been possible for the Neogene fossil record of soils (Retallack, 2022a).

CONCLUSIONS

Paleosols are now evidence for progressive CO_2 and CH_4 greenhouse reduction by biologically enhanced weathering to offset increased stellar luminosity and continued volcanic greenhouse gas emission. Biological regulation of soil and atmospheric gases may have maintained habitable surface conditions on Earth for the past 3.7 Ga.

ACKNOWLEDGMENTS

This work is a compilation of research from NSF grants EAR7900898, EAR850323, EAR9103178, OPP931522, SBR9513175, EAR0000953, and OPP023008, and PRF of American Chemical Society grants 31270 and 45257. Nathan Sheldon, Jim Kasting, and Paul Knauth offered useful discussion.

REFERENCES CITED

Battistuzzi, F.U., and Hedges, S.B., 2009, A major clade of prokaryotes with ancient adaptations to life on land: Molecular Biology and Evolution, v. 26, p. 335–343, https://doi.org/10.1093/molbev/msn247.

Beck, C., Grieser, C.J., and Rudolf, B., 2005, A new monthly precipitation climatology for the global land areas for the period 1951 to 2000: German Weather Service Offenbach Climate Status Report, v. 2004, p. 181–190.

Benison, K.C., and Bowen, B.B., 2015, The evolution of end-member continental waters: The origin of acidity in southern Western Australia: GSA Today, v. 25, no. 6, p. 4–10, https://doi.org/10.1130/GSATG231A.1.

Berner, R.A., 1997, The rise of plants and their effect on weathering and atmospheric CO_2: Science, v. 276, p. 544–546, https://doi.org/10.1126/science.276.5312.544.

Breecker, D.O., and Retallack, G.J., 2014, Refining the pedogenic carbonate atmospheric CO_2 proxy and application to Miocene CO_2: Palaeogeography, Palaeoclimatology, Palaeoecology, v. 406, p. 1–8, https://doi.org/10.1016/j.palaeo.2014.04.012.

Brimhall, G.H., Chadwick, O.A., Lewis, C.J., Compston, W., Williams, I.S., Danti, K.J., Dietrich, W.E., Power, M.E., Hendricks, D., and Bratt, J., 1992, Deformational mass transport and invasive processes in soil evolution: Science, v. 255, p. 695–702, https://doi.org/10.1126/science.255.5045.695.

Cawood, P.A., and Hawkesworth, C.J., 2019, Continental crustal volume, thickness and area, and their geodynamic implications: Gondwana Research, v. 66, p. 116–125, https://doi.org/10.1016/j.gr.2018.11.001.

Ciais, P., and 14 others, 2014, Carbon and other biogeochemical cycles, *in* Stocker, T., ed., Climate Change 2013: The Physical Science Basis: Cambridge, UK, Cambridge University Press, p. 465−570.

Dorozhkin, S.V., 2012, Dissolution mechanism of calcium apatites in acids: A review of literature: World Journal of Methodology, v. 2, p. 1–17, https://doi.org/10.5662/wjm.v2.i1.1.

Elberling, B., Askær, L., Jørgensen, C.J., Jönsen, H.P., Kühl, M., Glud, R.N., and Lauritsen, F.R., 2011, Linking soil O_2, CO_2, and CH_4 concentrations in a wetland soil: Implications for CO_2 and CH_4 fluxes: Environmental Science & Technology, v. 45, p. 3393–3399, https://doi.org/10.1021/es103540k.

Haqq-Misra, J.D., Domagal-Goldman, S.D., Kasting, P.J., and Kasting, J.F., 2008, A revised hazy methane greenhouse for the Archean Earth: Astrobiology, v. 8, p. 1127–1137, https://doi.org/10.1089/ast.2007.0197.

Kasting, J.F., 2010, Faint young Sun redux: Nature, v. 464, p. 687–689, https://doi.org/10.1038/464687a.

Kump, L.R., 2014, Hypothesized link between Neoproterozoic greening of the land surface and the establishment of an oxygen-rich atmosphere: Proceedings of the National Academy of Sciences of the United States of America, v. 111, p. 14,062–14,065, https://doi.org/10.1073/pnas.1321496111.

Kyaw Tha Paw, U., Xu, L., Ideris, A.J., Kochendorfer, J., Wharton, S., Rolston, D.E., and Hsia, T.C., 2006, Simultaneous carbon dioxide and oxygen measurements to improve soil efflux estimates: Kearney Foundation of Soil Science Final Report 2004211, p. 1–8.

Laakso, T.A., and Schrag, D.P., 2019, Methane in the Precambrian atmosphere: Earth and Planetary Science Letters, v. 522, p. 48–54, https://doi.org/10.1016/j.epsl.2019.06.022.

Lovelock, J.E., and Margulis, L., 1974, Atmospheric homeostasis by and for the biosphere: The Gaia hypothesis: Tellus, v. 26, p. 2–10, https://doi.org/10.3402/tellusa.v26i1-2.9731.

Markewich, H.W., Pavich, M.J., and Buell, G.R., 1990, Contrasting soils and landscapes of the Piedmont and Coastal Plain, eastern United States: Geomorphology, v. 3, p. 417–447, https://doi.org/10.1016/0169-555X(90)90015-I.

Marty, B., Zimmermann, L., Pujol, M., Burgess, R., and Philippot, P., 2013, Nitrogen isotope composition and density of the Archean atmosphere: Science, v. 342, p. 101–104, https://doi.org/10.1126/science.1240971.

Neaman, A., Chorover, J., and Brantley, S.L., 2005, Implications of the evolution of organic acid moieties for basalt weathering over geological time: American Journal of Science, v. 305, p. 147–185, https://doi.org/10.2475/ajs.305.2.147.

Pekkarinen, L.J., 1979, The Karelian formations and their depositional basement in the Kiihetelysvaar-Värtsilä area, east Finland: Geological Survey of Finland Bulletin, v. 301, p. 1–141.

Retallack, G.J., 2005, Pedogenic carbonate proxies for amount and seasonality of precipitation in paleosols: Geology, v. 33, p. 333–336, https://doi.org/10.1130/G21263.1.

Retallack, G.J., 2013, Ediacaran life on land: Nature, v. 493, p. 89–92, https://doi.org/10.1038/nature11777.

Retallack, G.J., 2018, Oldest recognized paleosols on Earth, Panorama Formation (3.46 Ga), Western Australia: Palaeogeography, Palaeoclimatology, Palaeoecology, v. 489, p. 230–248, https://doi.org/10.1016/j.palaeo.2017.10.013.

Retallack, G.J., 2022a, Soil carbon dioxide planetary thermostat: Astrobiology, v. 22, p. 116–123, https://doi.org/10.1089/ast.2020.2415.

Retallack, G.J., 2022b, Ordovician-Devonian lichen canopies before evolution of woody trees: Gondwana Research, v. 106, p. 211–223, https://doi.org/10.1016/j.gr.2022.01.010.

Retallack, G.J., 2022c, Soil salt and microbiome diversification over the past 3700 million years: Palaeogeography, Palaeoclimatology, Palaeoecology, v. 598, 111016, https://doi.org/10.1016/j.palaeo.2022.111016.

Retallack, G.J., Krinsley, D.H., Fischer, R., Razink, J.J., and Langworthy, K.A., 2016, Archean coastal-plain paleosols and life on land: Gondwana Research, v. 40, p. 1–20, https://doi.org/10.1016/j.gr.2016.08.003.

Retallack, G.J., Chen, Z.Q., Huang, Y., and Fang, Y., 2021, Oxidizing atmosphere and life on land during the late Paleoproterozoic outset of the "boring billion": Precambrian Research, v. 364, 106361, https://doi.org/10.1016/j.precamres.2021.106361.

Ribas, I., 2009, The Sun and stars as the primary energy input in planetary atmospheres: Proceedings of the International Astronomical Union, v. 5, p. 3−18, https://doi.org/10.1017/S1743921309992298.

Rye, R., and Holland, H.D., 1998, Paleosols and the evolution of atmospheric oxygen: A critical review: American Journal of Science, v. 298, p. 621–672, https://doi.org/10.2475/ajs.298.8.621.

Schwartzmann, D.W., 2017, Life's critical role in the long-term carbon cycle: The biotic enhancement of weathering: AIMS Geosciences, v. 3, p. 216–238, https://doi.org/10.3934/geosci.2017.2.216.

Sheldon, N.D., 2006, Precambrian paleosols and atmospheric CO_2 levels: Precambrian Research, v. 147, p. 148–155, https://doi.org/10.1016/j.precamres.2006.02.004.

Sheldon, N.D., and Retallack, G.J., 2001, Equation for compaction of paleosols due to burial: Geology, v. 29, p. 247–250, https://doi.org/10.1130/0091-7613(2001)029<0247:EFCOPD>2.0.CO;2.

Sheldon, N.D., Retallack, G.J., and Tanaka, S., 2002, Geochemical climofunctions from North American soils and application to paleosols across the Eocene-Oligocene boundary in Oregon: The Journal of Geology, v. 110, p. 687–696, https://doi.org/10.1086/342865.

Som, S.M., Buick, R., Hagadorn, J.W., Blake, T.S., Perreault, J.M., Harnmeijer, J.P., and Catling, D.C., 2016, Earth's air pressure 2.7 billion years ago constrained to less than half of modern levels: Nature Geoscience, v. 9, p. 448–451, https://doi.org/10.1038/ngeo2713.

Walker, J.C., 1982, Climatic factors on the Archean Earth: Palaeogeography, Palaeoclimatology, Palaeoecology, v. 40, p. 1–11, https://doi.org/10.1016/0031-0182(82)90082-7.

Wordsworth, R., and Pierrehumbert, R., 2013, Hydrogen-nitrogen greenhouse warming in Earth's early atmosphere: Science, v. 339, p. 64–67, https://doi.org/10.1126/science.1225759.

Manuscript received 15 Apr. 2022
Revised manuscript received 10 June 2022
Manuscript accepted 17 June 2022